24th INTERNATIONAL CONGRESS ON SOUND AND VIBRATION
23–27 July 2017, London

A NEW METHOD OF CONTROLLING FLUTTER OF CASCADE BLADES BASED ON A THREE-DIMENSIONAL MODEL

Xiaoyu Wang, Ruwen Qu and Xiaofeng Sun

Beihang University, School of Energy and Power Engineering, Beijing, PR China
email: bhwxy@buaa.edu.cn

The method of controlling flutter by using a non-rigid wall which has been verified feasible has unique advantages. However, the existence of soft wall section can destroy the continue boundary condition. In this paper, we develop a new method--transfer element method to tackle this problem by dividing the blade row and liner section as independent elements, respectively. For the blade row section, the blade unsteady forces assumed as dipoles source can be calculated by using the lifting surface theory. For the liner section, to avoid getting into the trouble of solving a complicated eigenvalue function, the method of equivalent source surface will play a positive role in tackling such issues by regarding lining walls as series of monopole sources. According to the pressure and axial velocity continuity conditions on the cross-section, we can obtain the algebraic equations expressed as a matrix expression which can be solved to obtain the unknown coefficients. It can be found that the change of admittance will result in significant changes in not only lift coefficient but also moment coefficient which can be cited to determine whether a blade flutters or not.
Keywords: cascade oscillation, transfer element method, lifting surface method

1. Introduction

During the past few decades, various approaches of passive flutter control techniques for turbomachinery rotors hold the promise in controlling various types of flutter. The proposed methods can be summarized into three main categories 1) mistuning, 2) aero-elastic tailoring, 3) dry friction and mode shape control. In addition to the above method, a novel way of suppressing blade flutter by using casing treatment has been verified by numerous researchers. Watanabe and Kaji [1] used a three-dimensional semi-actuator disk model to investigate the effects of a non-rigid wall on the aerodynamic damping, which can influence the aero-elastic stability of the blade. Guided by the method of equivalent source surface [2], Namba, Yamasaki and Kurihara [3] treated the non-rigid wall as a series of monopole sources, and the effects of the non-rigid wall was obtained by solving three-dimensional linearized Euler Equations under a hard wall boundary condition. Both of their studies have showed that a soft wall can influence aero-elastic stability to a certain degree. Recently the active control method has gained some achievements on this problem. An adjustable-wall-impedance model presented by Sun [4] can realize the active control. It has been known that non-rigid wall boundary condition takes effect on the flow field or acoustic field by the variation of the eigenvalues. Hence the core of the method is how to calculate the eigenvalues for a lined duct which is a thorny problem for a long time. Furthermore, the typical cascade flutter problem generally occurs in compressors or turbines so we should focus on three-dimensional annular duct. However, the blade rows in the above models including the adjustable-wall -impedance model are still placed between two parallel walls with infinite-length casing treatment. So a three-dimensional annular duct model will be required inevitably to realize the control of blade flutter.

In turbomachines, cascade flutter is in general characterized by the inter-blade phase angle of oscillation which means that the neighboring blade rows can influence the unsteady aerodynamic force via the aero-acoustic interaction between blade rows. Inspired by the fact, the interaction of a neighboring liner section on oscillating blades will be a critical factor for controlling effect. So it is of great importance to take such interaction mechanism into consideration. The theory of the transfer element method (TEM) proposed by Wang [5] which is just focused on this problem has been proved is a reliable technique to cope with the interaction between different acoustic element. The relevant work has been paid attention by Yang [6]. Based on the transfer element method, the aero-elastic model is developed by considering finite-length casing treatment. However, the wall surface remain be considered as two parallel walls. In order to destroy such limitation, in this paper the solution will be extend to a three dimensional annular duct with finite acoustic treatment length.

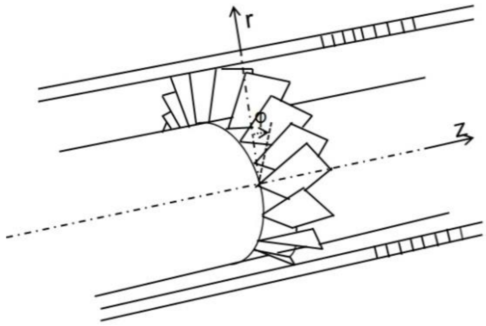

Figure 1: Analysis model included a liner section of finite length in an infinite duct

As shown in Fig.1, a model based on the transfer element method is constructed to investigate how a liner section will control blade flutter in a three-dimensional annular duct with a subsonic flow field. First, our model is comprised of two parts: blade row section and liner section. For the blade row section, given a known mode of blade vibration, the lifting surface theory suggested by Namba [7] can be utilized to calculate the intensity of the sound sources. Then the generated sound waves are expressed as a form of corresponding acoustic modal superposition. For a liner duct, the existing method of equivalent source surface is still an effective tool for obtaining the sound field in the duct. Secondly, the mode-match approach will be used to connect both elements. Then as we expected, we can get a matrix expression combined the two elements for all unknowns which have been given on the interface plane. Finally some numerical cases have been done here. The results indicate that the variation of wall boundary condition will result in significant changes of unsteady aerodynamic damping which is essence of this problem.

2. Mathematical mode

2.1 The lifting surface theory

For a rotor blade, the loading on the blade surface can be treated as diploe source. Considering that the $s(\vec{y})$ stands for surface area, the perturbation pressure induced by the oscillating blades can be shown as

$$p'(\vec{x},t)=\int_{-T}^{T}\int_{s(\tau)}\triangle\hat{p}_i\frac{\partial G}{\partial y_i}ds(\vec{y})d\tau \tag{1}$$

Now taking into account for all the blades, the total sound field in the duct can be shown as

$$\begin{aligned}p'_q(\vec{x},t)=&\frac{-i}{4\pi^2}\sum_{m=-\infty}^{\infty}\sum_{n=1}^{\infty}\frac{\psi_m(r)e^{im\varphi}}{\Gamma_m}\int_{s(\tau)}\sum_{k=1}^{B}\triangle p\psi_m(\overline{r'})e^{-im\varphi'}e^{-im(\overline{\varphi'}-\frac{2\pi}{B}(k-1))}\cdot e^{i(k-1)\sigma}\\&\int_{-\infty}^{\infty}e^{i\omega t}\int_{-\infty}^{\infty}(\frac{m}{\overline{r'}}-\alpha\frac{\Omega\overline{r'}}{U})\frac{e^{i\alpha(z-\overline{z'})}}{\beta^2\alpha^2-2Mk_0\alpha-k_0^2+k^2}\int_{-T}^{T}e^{i(-\omega+m\Omega+\Omega_s)\tau}d\tau d\omega d\alpha ds(\vec{y})\end{aligned} \tag{2}$$

Considering the basic fact

$$\sum_{k=1}^{B} e^{-im(\bar{\varphi}'-\frac{2\pi}{B}(k-1))}\cdot e^{i(k-1)\sigma}=\begin{cases}B & \sigma\frac{B}{2\pi}+m=sB\\ 0 & \sigma\frac{B}{2\pi}+m\neq sB\end{cases}\Rightarrow\quad m=sB-\sigma\frac{B}{2\pi} \tag{3}$$

Let $V=\sigma\frac{B}{2\pi}$ as an integer to represent the inter-blade phase parameter. According to the residue theorem and the momentum equation, the normal perturbation velocity will be finally got as:

$$\begin{aligned} v'_{\varphi''}=&\frac{-Be^{i\lambda t}}{2\pi\rho W}\sum_{s=-\infty}^{\infty}\sum_{n=1}^{\infty}\phi_{mn}(k_{mn}\bar{r})e^{im\bar{\varphi}_0}\int_{s(\tau)}\triangle p\phi_{mn}(k_{mn}\bar{r}')e^{-im\bar{\varphi}'_0}\\ &\left\{H(\bar{z}-\bar{z}')\left[\frac{\beta^2Me^{im\frac{\Omega}{U}(\bar{z}-\bar{z}')}e^{i\alpha_1(\bar{z}-\bar{z}')}}{2\kappa_{n,m}(M\kappa_{n,m}-k_0)}(\frac{m}{\bar{r}'}-\alpha_1\frac{\Omega\bar{r}'}{U})(\frac{m}{\bar{r}}-\alpha_1\frac{\Omega\bar{r}}{U})\right.\right.\\ &\left.+\frac{M^2e^{im\frac{\Omega}{U}(\bar{z}-\bar{z}')}e^{i\alpha_3(\bar{z}-\bar{z}')}}{k_0^2+M^2k_{m,n}^2}(\frac{m}{\bar{r}'}-\alpha_3\frac{\Omega\bar{r}'}{U})(\frac{m}{\bar{r}}-\alpha_3\frac{\Omega\bar{r}}{U})\right]\\ &\left.-H(z'-z)\frac{\beta^2Me^{im\frac{\Omega}{U}(\bar{z}-\bar{z}')}e^{i\alpha_2(\bar{z}-\bar{z}')}}{2\kappa_{n,m}(k_0+M\kappa_{n,m})}(\frac{m}{\bar{r}'}-\alpha_2\frac{\Omega\bar{r}'}{U})(\frac{m}{\bar{r}}-\alpha_2\frac{\Omega\bar{r}}{U})\right\}ds(\vec{y})\end{aligned} \tag{4}$$

where

$$\alpha_1=\frac{Mk_0-\sqrt{k_0^2-\beta^2k^2}}{\beta^2} \tag{5}$$

$$\alpha_2=\frac{Mk_0+\sqrt{k_0^2-\beta^2k^2}}{\beta^2} \tag{6}$$

$$\alpha_3=-\frac{\omega}{U} \tag{7}$$

$$\kappa_{n,m}=\begin{cases}\sqrt{k_0^2-\beta^2k_{m,n}^2} & k_0^2>\beta^2k_{m,n}^2\\ i\sqrt{\beta^2k_{m,n}^2-k_0^2} & k_0^2<\beta^2k_{m,n}^2\end{cases} \tag{8}$$

Based on the lifting-surface method, the eigenfunction can be expanded as the form of $\phi_m(k_{mn}r)=\sum_{l=1}^{L}B_{n,l}^{m}\phi_0(k_{0l}r)$, then the the integral function can be expressed as:

$$v'_{\varphi''}=\int_{s(\tau)}\triangle p\cdot(K_1+K_2+K_3)ds(\vec{y}) \tag{9}$$

K_1, K_2 and K_3 denote the downstream pressure wave kernel function, upstream pressure wave kernel function, and vortex wave kernel function successively and the expression of the kernel function can be expressed as

$$\begin{aligned}K_{1,2}=&\frac{-B}{2\pi\rho W}\sum_{l=1}^{L}r\phi_0(k_{0l}r)\sum_{l'=1}^{L}r'\phi_0(k_{0l'}r')\sum_{s=-\infty}^{\infty}\sum_{n=1}^{\infty}e^{im\varphi_0}e^{-im\varphi'_0}\\ &\frac{\beta^2Me^{im\frac{\Omega}{U}(z-z')}e^{i\alpha_{1,2}(z-z')}}{2\kappa_{n,m}[M\kappa_{n,m}\operatorname{sgn}(z-z')-k_0]}(mC_{n,l}^{m}-\alpha_{1,2}\frac{\Omega}{U}B_{n,l}^{m})(mC_{n,l'}^{m}-\alpha_{1,2}\frac{\Omega}{U}B_{n,l'}^{m})\end{aligned} \tag{10}$$

$$K_3 = \frac{-B}{2\pi\rho W}\sum_{l=1}^{L} r\phi_0(k_{0l}r)\sum_{l'=1}^{L} r'\phi_0(k_{0l'}r')\sum_{s=-\infty}^{\infty}\sum_{n=1}^{\infty} e^{im\varphi_0}e^{-im\varphi_0'}$$
$$H(z-z')\frac{M^2 e^{im\frac{\Omega}{U}(z-z')}e^{i\alpha_3(z-z')}}{k_0^2+M^2k_{m,n}^2}(mC_{n,l}^m-\alpha_3\frac{\Omega}{U}B_{n,l}^m)(mC_{n,l'}^m-\alpha_3\frac{\Omega}{U}B_{n,l'}^m) \quad (11)$$

Because of the rigidity of the blade, the normal perturbation velocity must be satisfied with the no penetration condition in the form as

$$v'_{\varphi''}+w'_{i,\varphi''}=0 \quad (12)$$

To solve the Eq.(12), the expansion technique is used here to tackle the unsteady forces Δp.Considering the distribution of the unsteady forces in new coordinate axis ϑ' and r' which can be converted from z' and r'.So the distribution of the unsteady forces can be expressed as:

$$\Delta p = \sum_{j'=1}^{J}\phi_{0j'}(r'_{\bar{j}})\left[A_{1j'}\cot\frac{\vartheta'}{2}+\sum_{i'=2}^{I}A_{i'j'}\sin(i'-1)\vartheta'_{\bar{i}}\right] \quad (13)$$

where

$$z'=\frac{b}{2}(1-\cos\vartheta');\ z=\frac{b}{2}(1-\cos\vartheta),\quad z,z'\in(0,b);\ \vartheta,\vartheta\in(0,\pi)\quad dz'=\frac{b}{2}\sin\vartheta' d\vartheta'$$
$$r'_{\bar{j}}=R_h+(R_d-R_h)\cdot\frac{\bar{j}-1}{\bar{J}-1};\quad \bar{j}=1,2,\cdots,\bar{J}\qquad \theta'_{\bar{i}}=\frac{\bar{i}\pi}{\bar{I}};\quad \bar{i}=1,2,\cdots,\bar{I} \quad (14)$$

Then the integral function can be written as a series of equation sets

$$w'_{ij}=\sum_{i'=1}^{I}\sum_{j'=1}^{J}A_{i'j'}\cdot\Im_{v(ij,i'j')}\qquad j'=1,2,\cdots,J' \quad (15)$$

where

$$\Im_{v(ij,i'j')}=-\Big\{K^{\nabla}_{ij,i'j'}(r_j,\cos\vartheta_i)+\sum_{l=1}^{L}r_j\phi_0(k_{0l}r_j)\cdot Q_{l,l'}\cdot\sum_{k'=1}^{K'_{num}}\frac{\pi}{K'_{num}}\left[S_{i,k'}-\log\left|\cos\vartheta'_{k'}-\cos\vartheta_i\right|\right]\Big\} \quad (16)$$

$$Q_{l,l'}=\frac{B}{2\pi\rho W}\frac{b}{2}\sum_{n=1}^{\infty}B_{n,l}^{\infty}B_{n,l'}^{\infty}\frac{i\lambda K_{m,n}^2}{BU\hat{K}_{m,n}} \quad (17)$$

$$K^{\nabla}_{ij,i'j'}(r_j,\cos\vartheta_i)=\int_0^{\pi}K^{\Delta}_{ij,j'}\cdot f'_{i'}(\vartheta')\frac{b}{2}d\vartheta' \quad (18)$$

2.2 The transfer element method

The model shown in Fig.2 is combined by a rotor blade row section and a liner section. In the rotor blade row section, in addition the reflecting waves $p'_{A,1}$, $p'_{B,1}$ and $w'_{A,1}$, there are also scattering pressure waves p'_s and vortex wave w'_s.

In order to construct a transfer element for a rotor blade, the key lies in how to express the scattering waves as the explicit function of standing waves. As shown in Fig.2, The standing wave can be obtained as

$$p'_{A,1}=\sum_{m=-\infty}^{\infty}\sum_{\mu=1}^{\infty}A_{m\mu}^{P}\cdot\phi_m(k_{m\mu}r)\cdot e^{i\alpha_1 z}\cdot e^{im\varphi} \quad (19)$$

where $A_{m\mu}^{P}$ is modal expansion coefficient.

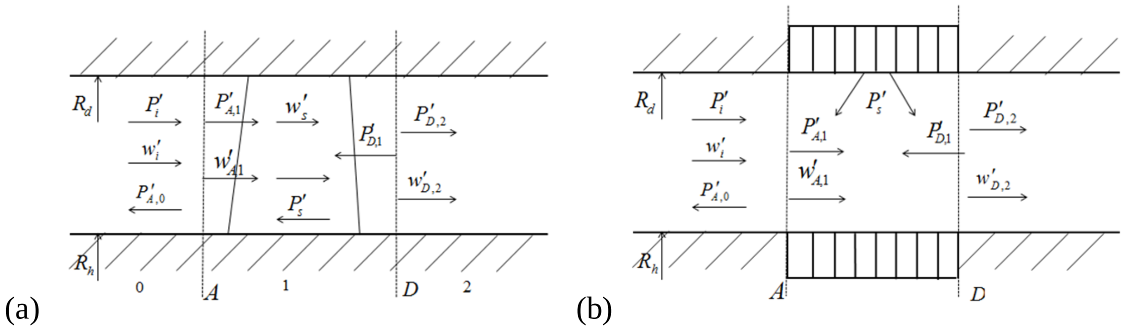

Figure 2: Analysis model: (a) the blade row section model in an infinite model, (b) the model for an acoustic liner section in an infinite duct

According to the lifting-surface method introduced in the preceding section, the scattering wave on interface A caused by the wave $p'_{A,1}$ can be expressed as

$$p'^{A_p}_{s,a-a}(r) = \sum_{n=1}^{\infty} \phi_{m'n}(k_{m'n} r) \sum_{i} \sum_{j} \left[\sum_{q=-\infty}^{\infty} \sum_{\mu=1}^{\infty} A^{p}_{m\mu} \cdot \aleph^{1}_{ij,q\mu} \right] \cdot \Re^{m'n,1}_{ij} \tag{20}$$

where

$$\aleph^{1}_{ij,q\mu} = \sum_{j'=1}^{J} \phi_{0j'}(r'_j) \left[\aleph'^{1}_{1j',q\mu} \cdot \cot\frac{\vartheta'_i}{2} + \sum_{i'=2}^{I} \aleph'^{1}_{i'j',q\mu} \cdot \sin(i'-1)\vartheta'_i \right] \tag{21}$$

$$\Re^{m'n,1}_{ij} = \frac{-B}{4\pi} \frac{\phi_{m'n}(k_{m'n} r'_j)}{\kappa_{n,m'}} \left(\frac{m'}{r'_j} - \alpha_1 \frac{\Omega r'_j}{U} \right) e^{-i\alpha_1 z'_i} e^{-i\frac{m'\Omega}{U} z'_i} \frac{\pi}{I} \frac{R_d - R_h}{J} \tag{22}$$

In this way, the other scattering wave can also be obtained as the form of modal expansion coefficient. As to the liner section the standing wave p' can be expressed as

$$P' = P_D' + P_A' = \sum_{m=-\infty}^{\infty} \sum_{\mu=1}^{\infty} D^{P}_{m\mu} \cdot \phi_{m,\mu}(k_{m,\mu} r) \cdot e^{i\alpha_2 z} \cdot e^{im\varphi} + \sum_{m=-\infty}^{\infty} \sum_{\mu=1}^{\infty} A^{P}_{m\mu} \cdot \phi_{m,\mu}(k_{m,\mu} r) \cdot e^{i\alpha_1 z} \cdot e^{im\varphi} \tag{23}$$

Inspired by the equivalent surface source method, we regard the wall admittance as series of monopole sources. So the disturbance wave p'_s can be expressed as

$$p'_s = \frac{\rho}{2} \sum_{m=-\infty}^{\infty} \sum_{n=-\infty}^{\infty} \frac{\Phi_{m,n}(x,y)}{\Gamma_{m,n}} \int_{s(\tau)} \Phi^{*}_{m,n}(x',y') V_n' \frac{\omega + U\gamma^{\pm}_{m,n}}{\kappa_{n,m}} e^{i\gamma^{\pm}_{m,n}(z-z')} ds(\vec{y}) \tag{24}$$

The corresponding boundary condition is

$$p'_s + Z_{zk} V^{f}_{n} = -p' \tag{25}$$

where V^f_n is the velocity perpendicular to liner surface, and Z_{zk} is non-dimensional characteristic impedance.

In order to describe the scattering waves in an explicit expression of wave coefficients $A^P_{m\mu}$ and $D^P_{m\mu}$, some special mathematical techniques is applied here. The details can be consulted from Ref. [6]. It can be proved that

$$p'_s = \frac{\rho}{2} \sum_{n} \frac{\phi_{mn}(k_{mn} r) \cdot e^{im\varphi} \cdot e^{i\alpha_{1,2}}}{2\pi} \left\{ \sum_{\mu} D^{P}_{m\mu} Q^{D^P_{m\mu}}_{n\pm} + A^{P}_{m\mu} Q^{A^P_{m\mu}}_{n\pm} \right\} \tag{26}$$

where $Q^{A^P_{m\mu}}_{n\pm}$ and $Q^{D^P_{m\mu}}_{n\pm}$ can also be referenced in Ref. [6].

Considering the pressure and axial velocity continuity conditions on the different cross-section, the transfer elements $B-C$ and $F-G$ denote a blade row section and a liner section, respectively. The related matrix equation can be written as

$$\begin{bmatrix} ss^{p_{A-A}}_{A^P_{m\mu}} & & & & & & & & \\ ss^{u_{A-A}}_{A^P_{m\mu}} & & & & & & & & \\ & B-C & & & & & & & \\ & & ss^{p_{d-d}}_{D^P_{m\mu}} & ss^{p_{d-d}}_{E^P_{m\mu}} & 0 & & & & \\ & & ss^{u_{d-d}}_{D^P_{m\mu}} & ss^{u_{d-d}}_{E^P_{m\mu}} & 0 & & & & \\ & & 0 & 0 & ss^{w_{d-d}}_{D^w_{0\mu}} & & & & \\ & & ss^{p_{e-e}}_{D^P_{m\mu}} & ss^{p_{e-e}}_{E^P_{m\mu}} & 0 & & & & \\ & & ss^{u_{e-e}}_{D^P_{m\mu}} & ss^{u_{e-e}}_{E^P_{m\mu}} & 0 & & & & \\ & & 0 & 0 & ss^{w_{e-e}}_{D^w_{0\mu}} & & & & \\ & & & & & F-G & & & \\ & & & & & & ss^{p_{h-h}}_{H^w_{m\mu}} & & \\ & & & & & & ss^{u_{h-h}}_{H^w_{m\mu}} & & \\ & & & & & & & ss^{w_{h-h}}_{w^w_{0\mu}} & \end{bmatrix} \begin{pmatrix} A^P_{m\mu} \\ B^P_{m\mu} \\ C^P_{m\mu} \\ B^w_{0\mu} \\ D^P_{m\mu} \\ E^P_{m\mu} \\ D^w_{0\mu} \\ F^P_{m\mu} \\ G^P_{m\mu} \\ F^w_{0\mu} \\ H^w_{m\mu} \\ H^w_{0\mu} \end{pmatrix} = \begin{pmatrix} 0 \\ 0 \\ 0 \\ I^P_{m\mu} \\ I^P_{m\mu} \\ I^w_{0\mu} \\ 0 \\ 0 \\ 0 \\ 0 \\ 0 \\ 0 \end{pmatrix} \quad (27)$$

3. Numerical results

3.1 Comparison with the existing numerical results

To validate our model, a comparison with the existing work [8] has been conducted. As mentioned in Ref. [8], we define the aerodynamic work as

$$W^*(r) = -\frac{i\pi}{2} R_d^2 \int_h^1 \sqrt{1+\left(\frac{\Omega r}{U}\right)^2} \int_{-b/2}^{b/2} \left[\bar{l}\cdot \vartriangle p - l \cdot \vartriangle \tilde{p}\right] dzdr \quad (28)$$

In this paper the blade displacement l composed of first order bending mode and first order torsion mode can be specified as

$$l(r,z) = H \cdot C_l \cdot h_l(r) \Big/ \sqrt{1+\left(\frac{\Omega r}{U}\right)^2} + \Theta \cdot \theta_\beta(r) \cdot (z - z_e) \cdot \sqrt{1+\left(\frac{\Omega r}{U}\right)^2} \quad (29)$$

H and Θ denote the translational displacement amplitude of the bending vibration and the angle displacement amplitude of torsion vibration, respectively. $h_1(r)$ and $\theta_\beta(r)$ denote the vibration mode of bending and torsion.

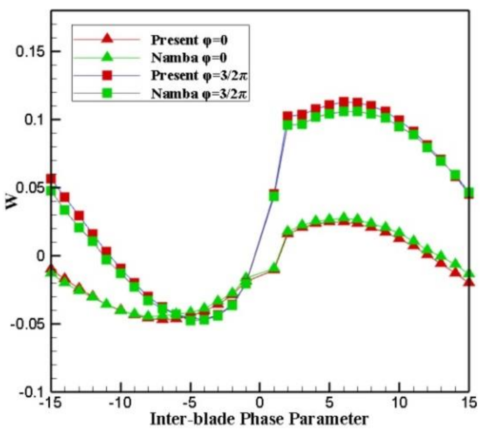

Figure 3: A Comparison with Namba's numerical results. $h = R_h / R_d = 0.4$, $M_t = 0.86604$, $M_r = 0.35$, $N_B = 30$, $\lambda = 0.1$, $H = 1$, $\Theta = e^{i\varphi}$

A case in Fig. 3 shows that the aerodynamic work coefficient varies with the inter-blade phase angle. The comparison between Namba's result and our model's under the same condition has showed a good agreement with each other. So our model is reliable in predicting the blade stability

3.2 Numerical results for a rotor blade row

For the final calculate, we define the lift coefficient and the moment coefficient for torsion vibration as:

$$C_L^t = \frac{1}{\bar{\rho} R_d \pi} \int_{R_h}^{R_d} \frac{\int_0^b \triangle p dz \sqrt{1+\frac{\Omega^2 r^2}{U^2}}}{U^2 \left(b \cdot \sqrt{1+\frac{\Omega^2 r^2}{U^2}} \right) \Theta} dr = \frac{1}{\bar{\rho} R_d \pi U^2 b \cdot \Theta} \int_{R_h}^{R_d} \int_0^b \triangle pdzdr \qquad (30)$$

$$C_M^t = \frac{1}{\bar{\rho} R_d \pi} \int_{R_h}^{R_d} \frac{\int_0^b \triangle p \cdot (z-z_e) dz \left[1+\frac{\Omega^2 r^2}{U^2} \right]}{U^2 \left(b \cdot \sqrt{1+\frac{\Omega^2 r^2}{U^2}} \right)^2 \Theta} dr = \frac{1}{\bar{\rho} R_d U^2 b^2 \pi \cdot \Theta} \int_{R_h}^{R_d} \int_0^b \triangle p \cdot (z-z_e) dzdr \qquad (31)$$

It can be seen that the change of the wall admittance can cause apparent effect on moment coefficient. As we all known, whether the blade flutter or not, it depends on the imaginary part of the moment coefficient, i.e. if the $C_{Mai}^t > 0$, the system become unstable, otherwise stable. In the paper, two cases are cited here to demonstrate the effect of casing treatment on aero-elastic stability. The moment coefficient of case one is plotted against the vibration of the inter-blade phase angle in Fig. 4. The Fig. 4 (a) stands for the real part of numerical results while the Fig. 4 (b) stands for the imaginary part.

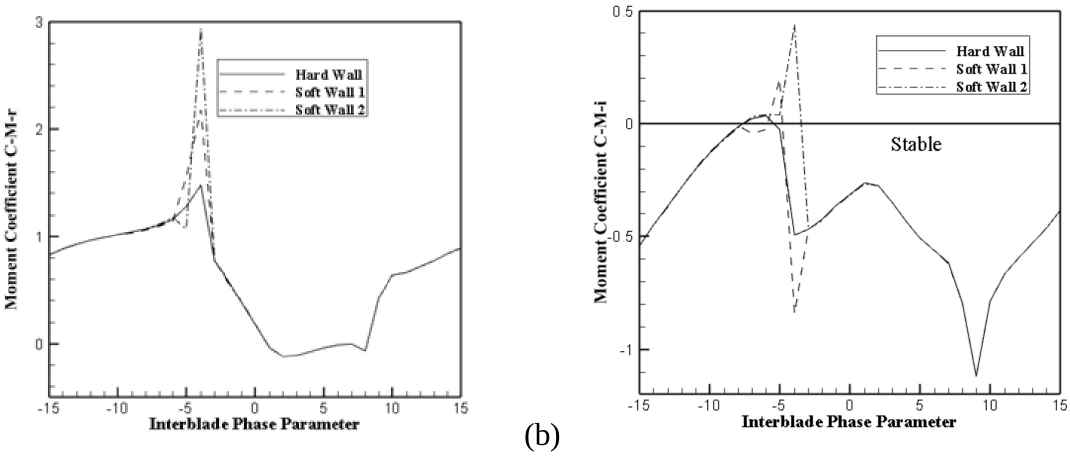

(a) (b)

Figure 4: Effect of inter-blade phase angle on the lift coefficient due to torsion motion: $h = R_h / R_d = 0.2$, $Rd = 1.0m$, $M_t = 0.86604, M_r = 0.35$, $N_B = 30$, $\Omega_s \cdot b = 0.28$, $\Theta = e^{i\varphi}$, $\varphi = -10^\circ$ .soft wall 1 $Z = (0.1, -2.0)$,soft wall 2 $Z = (0.1, -4.0)$

The case 1 is shown in Fig. 4. It can be noted that for hard wall boundary condition plotted in a solid line the system become stable expect the interval of inter-blade phase parameter around $\text{IBPP} = -7 \sim -6$, while the blade can become stable in the unstable interval by letting the impedance has the value of (0.1,-2.0). However, the original stable inter-blade phase parameters $\text{IBPP} = -5$become unstable under such boundary condition. When the value of the impedance is (0.1,-4.0), It is turn to inter-blade phase parameters $\text{IBPP} = -4$ become unstable. According to these plots the most striking feature is that the liner may play a counterproductive role on the aero-elastic stability, when the blade at some specific work conditions.

From the case 2 shown in Fig. 5, we can also conclude that the impedance will have a positive effect on the stability by letting the impedance has the value of (0.01, -1.7) when the inter-blade phase parameter $\text{IBPP} = -1$. On the other hand, if the impedance is adjust to (0.01, -4.0), the liner can play a counterproductive role on the aero-elastic stability of the inter-blade phase parameter $\text{IBPP} = -5$and $\text{IBPP} = -4$.

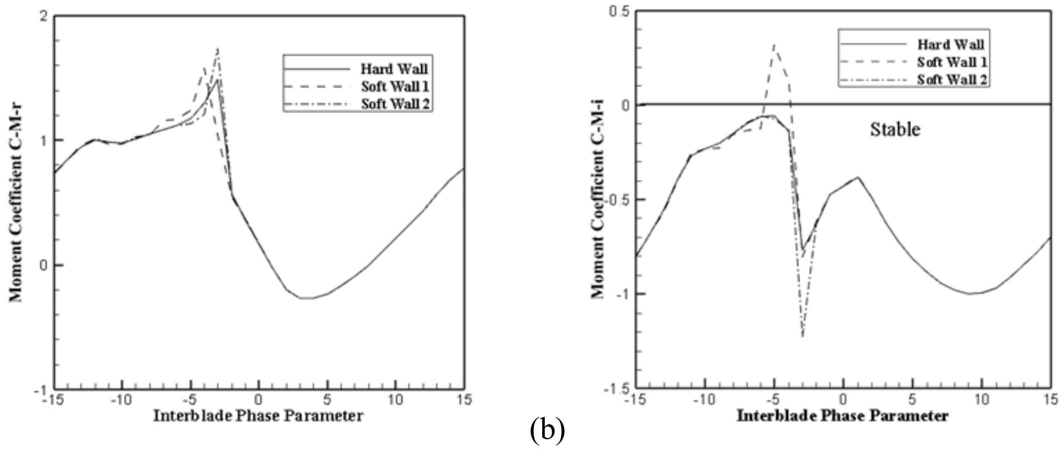

(a) (b)

Figure 5: Effect of inter-blade phase angle on the lift coefficient due to torsion motion: $h = R_h / R_d = 0.2$, $Rd = 1.0m$, $M_t = 0.86604$, $M_r = 0.3$, $N_B = 30$, $\Omega_s \cdot b = 0.3$, $\Theta = e^{i\varphi}$, $\varphi = -30^\circ$ .soft wall 1 $Z = (0.01, -1.7)$,soft wall 2 $Z = (0.01, -4.0)$

4. Conclusion

We have constructed a model based on the transfer element method to investigate how a liner section can control blade flutter in a three-dimensional annular duct with a subsonic flow field. In the present work, the effect of the liner on aero-elastic stability has been proved again. The most expressive phenomenon is that there is indeed some possibility of designing a liner to control blade flutter. Expect for some special conditions, the liner may have negative effect on suppressing blade flutter. The liner has already been applied to suppress noise in modern commercial aero-engine, however, it is crucial to insure the liner for suppressing noise has a positive effect on blade oscillation in the design stage.

REFERENCES

1 Watanabe, T., Kaji, S. Possibility of Cascade Flutter Suppression by Use of Non-rigid Duct Wall, *Proceedings Third International Symposium on Aeroelasticity in Turbomachines*, Cambridge, England, September (1984).

2 Namba, M., Fukushige, K. Application of the equivalent surface source method to the acoustics of duct systems with non-uniform wall impedance, *Journal of Sound and Vibration*, **73** (1), 125-146, (1980).

3 Namba, M., Yamsaki, N. and Kurihara, Y. Some Three-dimensional Effects on Unsteady Aerodynamic Forces on Oscillating Cascade. *Proceedings Third International Symposium on Aeroelasticity in Turbomachines*, Cambridge, England, September, (1984).

4 Sun, X., Kaji, S. Effects of Wall Admittance Changes on Aeroelastic Stability of Turbomachines, *AIAA Journal*, **38** (9), 1525-1533, (2000).

5 Wang, X., Sun, X. On the interaction of a fan stator and acoustic treatments using the transfer element method, *Fluid Dynamics Research*, **42** (1), 1-17, (2010).

6 Yang, Z., Wang, X. and Sun, X. Effect of finite-length casing treatment on cascade aero-elastic stability, *Journal of Aerospace Power*, **21**(6), 1027-1032, (2006)

7 Namba, M. Three-dimensional analysis of blade force and sound generation for an annular cascade in distorted flows, *Journal of Sound and Vibration*, **50** (4), 497-508, (1977)

8 Namba, M., Yamasaki, N. and Nishimura, S. Unsteady Aerodynamic Force on Oscillating Blades of Contra-rotating Annular Cascades, *Proceedings of 9th International Symposium on Unsteady Aerodynamics, Aeroacoustics and Aeroelasticity of Turbomachines*, Lyon, September, (2000)